

Non-equilibrium orbital edge magnetization

J. Voss,¹ I. A. Ado,¹ and M. Titov¹

¹*Radboud University, Institute for Molecules and Materials, NL-6525 AJ Nijmegen, The Netherlands*

Uncompensated non-equilibrium orbital magnetization may arise at sample edges in the presence of charge current. The value of the effect scales as the product of the current density and the electron mean free path without any additional smallness. This non-relativistic phenomenon originates in a lack of inversion symmetry of the electron wave functions in a vicinity of sample interfaces. In a conducting layer, where z direction is chosen perpendicular to the surface, and the current flows in x direction, the non-equilibrium orbital magnetization points in y direction. In a top-bottom symmetric layer, the orbital magnetization has an opposite sign near the top and bottom interfaces thus mimicking the symmetry of the spin-Hall effect but can exceed the latter by orders of magnitude.

The effects of orbital magnetization have been recently suggested to play a key role in many spintronics phenomena [1, 2]. Unlike magnetization arising from atomic magnetic moments in insulators, orbital magnetization in conductors may also be induced by circulating mesoscopic orbital currents that are not localized to atoms.

Circulating currents in diamagnetic conductors have been known since early days [3]. Even though such amperere currents are formally quite large their total effect on magnetization is cancelled out in thermodynamic equilibrium (with the exception of a persistent current in a nano-ring at ultra low temperatures [4]). The cancellation is a consequence of the dense (continuous) spectrum of the extended states in the band.

Below we argue that the finite orbital magnetization may nevertheless arise from extended states in non-equilibrium conditions. For a sample with charge current this leads to a finite orbital magnetization at sample surfaces. In this case the characteristic area circumvented by the uncompensated circulating orbital current scales as the square of the electron mean free path and is proportional to the value of the charge current applied.

The presence of charge current creates an unequal occupation of quasiparticle states with the momentum parallel and anti-parallel to the current direction. When such quasiparticles are reflected from a flat interface (that is parallel to the current) they turn different directions (clockwise or anti-clockwise) depending on the sign of the momentum projection on the interface. Unequal occupation of the left and right traveling states is, then, translated to the uncompensated orbital magnetic moment on the interface.

In this Letter we estimate the magnitude of the phenomenon using Landauer-Büttiker approach to charge transport [5]. Before we proceed with the estimate we pause to define the orbital moment density.

In thermodynamics we often consider the total magnetic moment of the system as a quantity that is dual to external magnetic field \mathbf{B} . For the differential of the grand potential we write $d\Omega = -\mathbf{M} \cdot d\mathbf{B}$, where \mathbf{M} is a total magnetic moment of the sample while $d\mathbf{B}$ is a differential of homogeneous external magnetic field. One may

naively generalize the relation to define magnetization as the functional derivative of the grand potential functional with respect to the local field $\mathbf{B}(\mathbf{r})$. Such definition is, however, unphysical because elementary magnetic field exists only in a form of a line and cannot be taken as a three dimensional delta function.

Nevertheless, one can define orbital moment density by considering a change of magnetic flux $d\Phi$ through a small two-dimensional area (a flux tube). In this case, the dual variable has a meaning of the two-dimensional (2D) orbital moment density (magnetic moment per 2D area in the plane perpendicular to the flux), $d\Omega = -\mathcal{M} \cdot d\Phi$. We use this relation to define the density \mathcal{M} of orbital magnetic moments.

For a sake of definiteness we consider a particular sample geometry illustrated in Fig. 1. The conducting layer of the thickness W in z direction has a large (formally unlimited) length L_y in y direction and the length L in x direction. The charge current is applied in x direction. In this geometry the non-equilibrium orbital magnetization, which points out in y direction, is formed on the top and bottom surfaces.

In order to define the orbital moment density we choose an external magnetic field B in the form of magnetic line

$$\mathbf{B} = \Phi_0 \hat{\mathbf{y}} \delta(x - x_0) \delta(z - z_0), \quad (1)$$

where $\hat{\mathbf{y}}$ is the unit vector in y direction and Φ_0 is the corresponding flux penetrating (x, z) cross-section. The corresponding vector potential takes the form

$$\mathbf{A}(\mathbf{r}) = \Phi_0 \left(\frac{1}{2\pi} \frac{(\mathbf{r} - \mathbf{r}_0) \times \hat{\mathbf{y}}}{|\mathbf{r} - \mathbf{r}_0| \times |\hat{\mathbf{y}}|^2} + \nabla \chi \right), \quad (2)$$

where χ is an arbitrary gauge field.

By computing the energy $E = \langle \Psi | H | \Psi \rangle$ in the presence of \mathbf{A} for a given state Ψ , we obtain y component of the corresponding orbital moment density as

$$\mathcal{M}(x_0, z_0) = - \left. \frac{\partial E}{\partial \Phi_0} \right|_{\Phi_0=0}. \quad (3)$$

By expanding the energy functional up to the linear order in \mathbf{B} one may show that the integration of the density \mathcal{M}

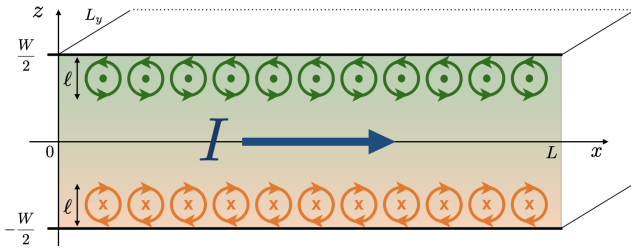


FIG. 1. Sketch of the sample geometry. Charge current flow in x direction is a cause of finite orbital moment density at the top and bottom interfaces. Electron quasiparticle states with $k_x > 0$ and $k_x < 0$ are unequally populated due to current. The number of interface reflections in which electron trajectory turns clock-wise or anti-clockwise around y direction are then also different. This translates into uncompensated orbital moment pointing out in y direction, which is formed within the layer of the order of mean free path from the surface. In a symmetric sample the effect has an opposite sign on the top and bottom interfaces.

over the cross-section coordinates (x_0, z_0) must return the definition of the full orbital moment of the sample

$$M = \int dx_0 dz_0 \mathcal{M}(x_0, z_0), \quad (4)$$

which is projected here on y direction.

The definition of Eq. (3) can be further generalized by replacing the energy with the grand potential for the ensemble of electronic states. This definition has a clear physical meaning. By selecting an axis (in y direction) with the coordinates x_0 and z_0 we count how all charges in the sample circulate around the axis to contribute to angular momentum along the axis.

We may now look at the conducting sample in an effective model description that fails to resolve individual atoms or atomic orbitals and operate, instead, on the electron envelope wave functions that are smooth on atomic scales. The most trivial effective Hamiltonian of that kind has a form of an effective Schrödinger equation $H\Psi = E\Psi$ with $H = (p - e\mathbf{A})^2/2m + V(\mathbf{r})$, where $e = -|e|$ is the electron charge, the speed of light is set to unity and V is an external or disorder potential. Here we assume the geometry of Fig. 1 with the boundary conditions $\Psi(z = \pm W/2) = 0$.

Using Landauer-Büttiker approach we may construct the density matrix for an open system with a charge current flow. We start by looking at the ballistic system, i. e. the system with no disorder $V = 0$. The population of quantum states in a system with current flow may be represented in terms of Landauer-Büttiker scattering states that originate in reservoirs with different chemical potentials. For a clean system we may define left- and

right-going scattering states as

$$\Psi_{n,s,>} = \sqrt{\frac{2}{WL_y v_x}} e^{ikx} e^{ip_s y} \cos(q_n z), \quad (5a)$$

$$\Psi_{n,s,<} = \sqrt{\frac{2}{WL_y v_x}} e^{-ikx} e^{ip_s y} \cos(q_n z), \quad (5b)$$

where $q_n = \pi(2n - 1)/W$ for $n = 1, 2, 3, \dots$. Such quantization follows from the hard-wall boundary conditions in z direction. In our model we have $v_x = \hbar k/m$ and $k = \sqrt{2mE/\hbar^2 - q_n^2 - p_s^2} > 0$. The scattering states yield the spectral equation $H\Psi = E\Psi$.

In this calculation we assume $L_y \gg W$, hence we may not worry about the boundary condition in y direction. Here we simply assume that those are periodic $\Psi(y = 0) = \Psi(y = L_y)$, hence $p_s = 2\pi s/L_y$ with an arbitrary integer s (negative, zero and positive). The scattering states in our setup are, therefore, numerated by two integer indexes n and s , where n is positive and s is arbitrary.

The scattering states are normalized to the unit charge current flux. The current in the state Ψ is defined as $\mathbf{J}[\Psi] = -ie\hbar(\Psi^\dagger(\nabla\Psi) - (\nabla\Psi^\dagger)\Psi)/2m$. For the scattering states it gives

$$J_x[\Psi_{>}] = -J_x[\Psi_{<}] = \frac{2e}{L_y W} \cos^2(q_n z). \quad (6)$$

The charge flux of the scattering state is given by

$$Q[\Psi] = \int_{-W/2}^{W/2} dz \int_0^{L_y} dy J_x[\Psi], \quad (7)$$

hence, indeed, we have $Q[\Psi_{>}] = e$ and $Q[\Psi_{<}] = -e$ as the normalization condition [6].

In the Landauer-Büttiker picture the scattering states are filled according to the population of energy levels in the left and right reservoirs. The states $\Psi_{>}$ are filled according the Fermi-Dirac distribution function $f_L(E)$, while the states $\Psi_{<}$ are filled according the Fermi-Dirac distribution function $f_R(E)$. Thus, we find the total current (from left to right) as

$$\begin{aligned} I &= \sum_{s,n} \int \frac{dE}{2\pi\hbar} (Q[\Psi_{n,s,>}] f_L(E) + Q[\Psi_{n,s,<}] f_R(E)) \\ &= e \int \frac{dE}{2\pi\hbar} (f_L(E) - f_R(E)) N(E). \end{aligned} \quad (8)$$

The quantity $N(E)$ counts the number of open channels, i. e. the number of possible choices for n and s such that k remains real,

$$N(E) = 2 \sum_{s=-\infty}^{\infty} \sum_{n=1}^{\infty} \Theta(q_n^2 + p_s^2 \leq 2mE/\hbar^2) = \frac{WL_y}{4\pi} k_F^2,$$

where $k_F^2 = 2mE/\hbar^2$ and the factor 2 takes care of the electron spin. The expression of Eq. (8) is nothing but the celebrated Landauer formula.

In the linear response one can use

$$f_L(E) - f_R(E) = f(E_F - eV_{\text{bias}}) - f(E_F) \approx eV_{\text{bias}} \left(-\frac{\partial f}{\partial E} \right),$$

where E_F is the Fermi energy and V_{bias} is the voltage bias applied. Furthermore, for any practical purpose we can use $-\partial f/\partial E = \delta(E - E_F)$ and obtain

$$I = \frac{e^2}{4\pi h} W L_y k_F^2 V_{\text{bias}} = \frac{e^2}{h} W L_y \nu E_F V_{\text{bias}}, \quad (9)$$

where $\nu = m/2\pi\hbar^2$ is the 2D density of states. Clearly $W L_y \nu E_F \gg 1$ is a dimensionless quantity that quantifies the sample conductance.

Following the same ideology we may also compute the uncompensated orbital moment density that arise in the presence of charge current. First of all we add the vector potential from Eq. (2) to the effective Hamiltonian using the Peierls substitution. The contribution to the electron free energy in the linear order with respect to the vector potential is given by

$$\delta\Omega = - \int d^3\mathbf{r} \mathbf{j}(\mathbf{r}) \cdot \mathbf{A}(\mathbf{r}), \quad (10)$$

where $\mathbf{j}(\mathbf{r})$ is the charge current density. We ignore here the diamagnetic term, which is proportional to A^2 , since we are interested in the orbital magnetization in the absence of external field (see Eq. (3)).

By differentiating $\delta\Omega$ with respect to Φ_0 (assuming $\Phi_0 = 0$) we obtain the orbital moment density as

$$\mathcal{M}(\mathbf{r}_0) = \int d^3\mathbf{r} \mathbf{j}(\mathbf{r}) \cdot \left(\frac{1}{2\pi} \frac{(\mathbf{r} - \mathbf{r}_0) \times \hat{\mathbf{y}}}{|(\mathbf{r} - \mathbf{r}_0) \times \hat{\mathbf{y}}|^2} + \nabla\chi \right), \quad (11)$$

where $\mathbf{r}_0 = (x_0, 0, z_0)$ specifies the axis. We see that the gauge field χ drops off the expression above due to the charge conservation. We may always perform the integration by parts and use $\nabla \cdot \mathbf{j} = 0$ for any \mathbf{j} that is computed on a spectral eigenstate. The integration by parts is justified since the current density is vanishing beyond the sample boundaries.

To define the total orbital momentum of the sample one may choose the vector potential in the symmetric gauge $\mathbf{A} = B \hat{\mathbf{y}} \times \mathbf{r}/2$, which corresponds to the homogeneous field $\mathbf{B} = B \hat{\mathbf{y}}$. The derivative of energy over B returns, then, the total moment in y direction as [7]

$$M = \frac{1}{2} \int d^3\mathbf{r} \hat{\mathbf{y}} \cdot [\mathbf{r} \times \mathbf{j}(\mathbf{r})]. \quad (12)$$

The definition of the total orbital moment (12) is notoriously difficult to apply in conducting samples due to the fact that the operator \mathbf{r} is unbounded [8, 9]. Regularization schemes have been suggested to overcome the problem [10–13]. In contrast the definition of orbital moment density (11) is well-defined and does not require any further regularization. Even though the relation of

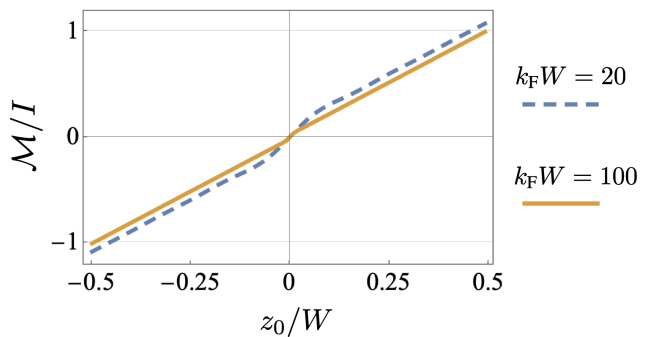


FIG. 2. The 2D orbital moment density profile from Eq. (15). The density is reaching the value I on the top and bottom interfaces. The effect of Friedel oscillations (described by J_1 function) is weak and vanishes in the limit $k_F W \gg 1$. In this limit one finds $\mathcal{M}(z_0) = 2I z_0/W$.

Eq. (4) must hold by construction, it may be violated in practice if the regularization of Eq. (12) does not respect the gauge symmetry.

The orbital moment density \mathcal{M} is measured in Amperes, i.e. in the units of charge current. Indeed, the magnetization units are A/m, hence the magnetic moment per length square correspond to Amperes. Since the current density \mathbf{j} is measured in Amperes per length square, the dimension of Eq. (11) is evidently correct. The magnetic moment M is measured in Amperes times the length squared.

In our setup we have $\mathbf{j} = j_x \hat{\mathbf{x}}$. To compute the expectation value of \mathcal{M} we have to use the same procedure as for the computation of current,

$$\begin{aligned} \mathcal{M} = & -2 \sum_{s,n} \int d^3\mathbf{r} \int \frac{dE}{2\pi\hbar} \frac{1}{2\pi} \frac{z - z_0}{(x - x_0)^2 + (z - z_0)^2} \\ & \times (f_L(E) J_x[\Psi_{n,s,>}] + f_R(E) J_x[\Psi_{n,s,<}]), \quad (13) \end{aligned}$$

where the overall factor 2 takes care of electron spin. In the other words, the result is obtained by summing up all contributions from all scattering states that are filled.

Using the result of Eq. (6) we find

$$\begin{aligned} \mathcal{M} = & \frac{-2e}{\pi h L_y W} \sum_{s,n} \int d^3\mathbf{r} \int dE (f_L(E) - f_R(E)) \\ & \times \frac{z - z_0}{(x - x_0)^2 + (z - z_0)^2} \cos^2(q_n z). \quad (14) \end{aligned}$$

Now we have to apply the definition of Eq. (9) and relate the density \mathcal{M} to the total current. We use again Eq. (9) to project on the Fermi level. The summation over the channels in Eq. (14) is performed as

$$\begin{aligned} & 2 \sum_{s=-\infty}^{\infty} \sum_{n=1}^{\infty} \cos^2(q_n z) \Theta(q_n^2 + p_s^2 \leq 2mE/\hbar^2) \\ & = \frac{L_y W}{4\pi} k_F^2 \left(1 + \frac{J_1(2k_F z)}{k_F z} \right) = N(E) \left(1 + \frac{J_1(2k_F z)}{k_F z} \right), \end{aligned}$$

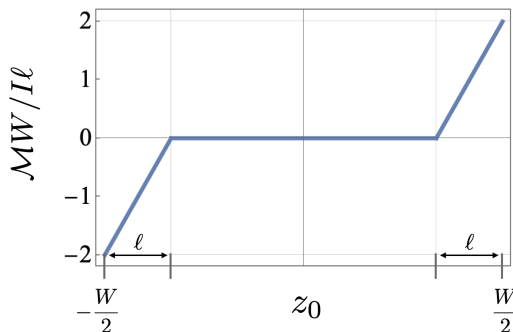


FIG. 3. The sketch of orbital moment density \mathcal{M} profile in the presence of disorder.

where $J_1(x)$ is the Bessel function. Thus we find

$$\mathcal{M} = -I \frac{1}{\pi W} \iint dx dz \left(1 + \frac{J_1(2k_F z)}{k_F z} \right) \times \frac{z - z_0}{(x - x_0)^2 + (z - z_0)^2}, \quad (15)$$

where we have also performed the integration over y . It is easy to see that the expression is almost independent on x_0 apart from the vicinity of edges in x direction. (We assume $L \gg W$ where L is the system length in x direction). The dependence on z_0 is illustrated in Fig. 2.

The Bessel function in Eq. (15) takes into account multiple reflections from the sample boundaries, which describe Friedel oscillations from the boundary. The relative contribution of the Friedel oscillations to the orbital moment density becomes, however, irrelevant for samples which are much wider than the Fermi wave length. For $L \gg W$ and $Wk_F \gg 1$, the result of Eq. (15) simplifies to $\mathcal{M}(x_0, z_0) = 2Iz_0/W$.

The total magnetic moment M is clearly vanishing in our system due to the exact top-bottom symmetry $z \rightarrow -z$, while the orbital moment density is finite. The finite value of the density is clearly related to the fact that current carrying wave functions are sensitive to sample edges and are not symmetric with respect to the top-bottom inversion. As the result the density reaches its maximal (though the opposite) values at the top and bottom interfaces.

Let us now speculate on the modification of the result of Eq. (15) in a more realistic case of a disordered system. In a disordered sample the wave-functions at a distance larger than the mean free path ℓ are not sensitive to the boundary condition, hence, they cannot contribute to the orbital moment density. Thus, the latter will be entirely determined by a layer of the order of the mean free path from the surface. Let us model the layer of the thickness ℓ near the interface as a ballistic sample but with the condition $\mathcal{M} = 0$ at the depth ℓ from the surface.

For $k_F \ell \gg 1$ the orbital moment density \mathcal{M} increases linearly from 0 at a distance ℓ from the surface to the

value $2I\ell/W$ at the surface (where I is the total current). Thus the total orbital magnetic moment of the surface layer is given by

$$M_{\text{edge}} = I\ell^2 L/W, \quad (16)$$

For this estimate we assume that the electron density is constant up to the sample boundary where it is abruptly vanishing. In semiconducting samples this may not be the case since the electron gas may be gradually depleted or populated in a vicinity of the surface, which might be an especially strong at the interface between two materials. The charge redistribution may change both the magnitude and even the sign of the orbital moment density at the surface and has to be analyzed separately.

For a disordered metallic sample the anticipated result is sketched in Fig. 3. The result of Eq. (16) scales as ℓ^2 which suggests that the orbital magnetic moment is accumulated from the characteristic area of ℓ^2 near the edge. This area is clearly much larger than the atomic cross-section which represents a notable difficulty for any ab initio (atomistic) approach to the phenomenon [13].

It may also be instructive to introduce the average current density \bar{j} instead of the total current $I = L_y W \bar{j}$ in order to rewrite the result of Eq. (16) as

$$M_{\text{edge}} = \bar{j} \ell^2 L L_y. \quad (17)$$

In terms of the standard magnetization (which is the ratio of the magnetic moment to the corresponding volume) we estimate the edge magnetization as

$$\mathcal{M}_{\text{edge}}^{3D} = \frac{M_{\text{edge}}}{L_y L \ell} = \bar{j} \ell, \quad (18)$$

which is a very large effect that contains no spin-orbit smallness. We note that Rashba-Edelstein and spin Hall effects [14–16], which have the same symmetry, do necessarily contain an additional small factor Δ_{so}/E_F and $(\Delta_{\text{so}}/E_F)^2$ respectively, where Δ_{so} is a spin-orbit splitting. This factor is of the order of $10^{-2} - 10^{-9}$ thus strongly suppressing the role of these effects.

The non-equilibrium orbital magnetization effect may also provide an alternative explanation to experimental observations that are currently attributed to the orbital Hall effect [17–21].

In conclusion we have considered orbital magnetic moment that arise at the surface of a conducting sample in the presence of parallel current flow. The effect is due to unequal number of surface reflections for quasi-particles with $k_x > 0$ and $k_x < 0$. The phenomenon does not rely upon any spin-orbit coupling. The effect is identical in symmetry to the spin-Hall or Rashba-Edelstein effects but exceeds those by orders of magnitude. The corresponding non-equilibrium edge magnetization can reach the value $\bar{j} \ell$ where ℓ is the electron mean free path and $\bar{j} = I/L_y W$ is the charge current density in the sample.

The effect depends on the quality of the interface and is suppressed for disordered interfaces. The effect provides an alternative explanation to the measurements that are currently attributed to the orbital Hall, Rashba-Edelstein and Spin-Hall effects. More detailed theory is, however, required to understand the role of possible electron density gradient at the surface and a similar effect that takes place in hydrodynamics regime due to formation of current vortices.

We appreciate discussions with Vladimir Bashmakov, Dimi Culcer, Rembert Duine, Ivan Iorsh, Yuri Mokrousov and Thierry Valet.

We acknowledge funding from the European Union's Horizon 2020 research and innovation programme under the Marie Skłodowska-Curie grant agreement No 873028.

-
- [1] D. Go, D. Jo, H.-W. Lee, M. Kläui, and Y. Mokrousov, *Europhysics Letters* **135**, 37001 (2021).
- [2] R. B. Atencia, A. Agarwal, and D. Culcer, "Orbital angular momentum of bloch electrons: equilibrium formulation, magneto-electric phenomena, and the orbital hall effect," (2024), arXiv:2403.07055 [cond-mat.mes-hall].
- [3] A. Einstein and W. J. de Haas, *Koninklijke Akademie van Wetenschappen te Amsterdam, Proceedings*. **18**, 696 (1915).
- [4] A. C. Bleszynski-Jayich, W. E. Shanks, B. Peaudecerf, E. Ginossar, F. von Oppen, L. Glazman, and J. G. E. Harris, *Science* **326**, 272 (2009), <https://www.science.org/doi/pdf/10.1126/science.1178139>.
- [5] Y. Blanter and M. Büttiker, *Physics Reports* **336**, 1 (2000).
- [6] The dimensions of $\mathbf{J}[\Psi]$ and $Q[\Psi]$ are different from those of \mathbf{j} and I , because we employ the continuous spectrum normalization of the scattering states. It is the integration of $\mathbf{J}f(E)$ or $Qf(E)$ over the energy divided by $2\pi\hbar$ that returns the current density and current, respectively.
- [7] Alternatively, one can use Landau gauge and define y -component of the total orbital moment as $M = \int d^3\mathbf{r}j_xz$ or $M = -\int d^3\mathbf{r}j_zx$.
- [8] L. L. Hirst, *Rev. Mod. Phys.* **69**, 607 (1997).
- [9] R. Resta, *Journal of Physics: Condensed Matter* **22**, 123201 (2010).
- [10] T. Thonhauser, D. Ceresoli, D. Vanderbilt, and R. Resta, *Phys. Rev. Lett.* **95**, 137205 (2005).
- [11] D. Xiao, J. Shi, and Q. Niu, *Phys. Rev. Lett.* **95**, 137204 (2005).
- [12] J. Shi, G. Vignale, D. Xiao, and Q. Niu, *Phys. Rev. Lett.* **99**, 197202 (2007).
- [13] T. Thonhauser, *International Journal of Modern Physics B* **25**, 1429 (2011), <https://doi.org/10.1142/S0217979211058912>.
- [14] V. Edelstein, *Solid State Communications* **73**, 233 (1990).
- [15] J. E. Hirsch, *Phys. Rev. Lett.* **83**, 1834 (1999).
- [16] J. Sinova, S. O. Valenzuela, J. Wunderlich, C. Back, and T. Jungwirth, *Rev. Mod. Phys.* **87**, 1213 (2015).
- [17] Y.-G. Choi, D. Jo, K.-H. Ko, D. Go, K.-H. Kim, H. G. Park, C. Kim, B.-C. Min, G.-M. Choi, and H.-W. Lee, *Nature* **619**, 52 (2023).
- [18] I. Lyalin, S. Alikhah, M. Berritta, P. M. Oppeneer, and R. K. Kawakami, *Phys. Rev. Lett.* **131**, 156702 (2023).
- [19] G. Sala, H. Wang, W. Legrand, and P. Gambardella, *Phys. Rev. Lett.* **131**, 156703 (2023).
- [20] H. Hayashi and K. Ando, *Applied Physics Letters* **123**, 172401 (2023), https://pubs.aip.org/aip/apl/article-pdf/doi/10.1063/5.0170654/18180679/172401_1_5.0170654.pdf.
- [21] Y.-G. Choi, D. Jo, K.-H. Ko, D. Go, K.-H. Kim, H. G. Park, C. Kim, B.-C. Min, G.-M. Choi, and H.-W. Lee, *Nature* **619**, 52 (2023).